JCTC Journal of Chemical Theory and Computation

Article

pubs.acs.org/JCTC

Hydration Free Energies of Multifunctional Nitroaromatic Compounds

Alauddin Ahmed and Stanley I. Sandler*

Department of Chemical and Biomolecular Engineering, University of Delaware, Newark, Delaware 19716, United States

Supporting Information

ABSTRACT: Nitroaromatic compounds (NACs) are used as energetic materials, reagents, and pesticides; however, they are potentially hazardous for the environment and human health. To predict the environmental distribution of these compounds, the vapor pressure, aqueous solubility, and Henry's law constant are important properties, as is the solvation free energy in water from which the latter two can be computed. Here, we have calculated the hydration free energies for a set of nine nitroaromatic compounds containing one, two, and three nitro groups using the expanded ensemble molecular dynamics simulation method with TIP3P water and the GAFF, CGenFF, OPLS-AA, and TraPPE force field parameters and the RESP (gas phase), CHELPG (gas phase), and CM4 (aqueous phase) partial atomic charges calculated here. Also, we have computed hydration free energies using the reported default partial atomic charges of the OPLS-AA force field and using the semiempirical AM1-BCC charges with GAFF parameters. The effect of water model flexibility on the computation of hydration free energy is examined with CGenFF/(CHELPG+SPC-Fw) model. All the force fields studied generally led to less accurate predictions with increasing numbers of nitro groups. The average unsigned errors (AUE) show that 6 of 16 force-field/(charge+water) models used perform approximately equally well in predicting measured hydration free energies: these are CGenFF/(CHELPG+TIP3P), CGenFF/(CM4+TIP3P), OPLS-AA/(CHELPG+TIP3P), OPLS-AA/(CM4+TIP3P), TraPPE-UA/(CHELPG+TIP3P), and TraPPE-UA/(CM4+TIP3P). When using the default atomic charges, the OPLS-AA force field was the most accurate, though using CHELPG and CM4 charges led to better predictions. Our analyses indicate that not only the charges but also the van der Waals interaction parameters for the nitro-group nitrogen and oxygen atoms in the force fields are partly responsible for the performance variations in predicting solvation free energies. We also compared the force field-based simulation results with the predictions from the SM6 solvation model and Abraham linear solvation energy relationship (LSER) method. With an appropriate choice of theory and basis set both for geometry optimization and computation, which unfortunately is not known *a priori*, the SM6 model hydration free energy predictions for the NACs are comparable to the simulation results here. The Abraham LSER predictions with descriptors obtained from the Platts method are of reasonable accuracy. A useful addition to this paper is the Supporting Information that contains a compiled and evaluated list of the hydration free energies of the NACs studied here assembled from the literature.

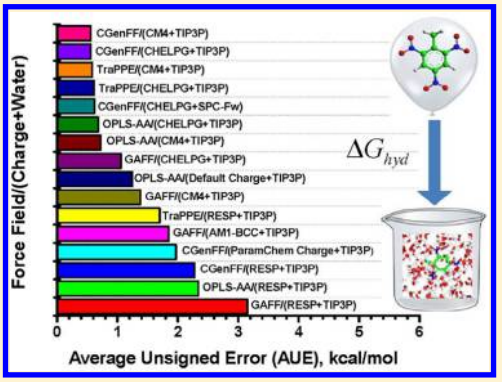

I. INTRODUCTION

Nitroaromatic compounds (NACs) are not abundant in nature but are synthesized for industrial applications. Over the past century, NACs have found applications in agriculture as herbicides and insecticides, as solvents, in dyes, in polyurethane foams, and as energetic materials in the military, in demolition, in the mining industry, and as rocket fuels. The NACs are classified as hazardous materials and potentially harmful to biological cells. Contamination by NACs in soil, sediment, and surface and groundwater, which is usually the result of water mediated transport, is found at military testing sites, war zones, mining areas, and demolition sites. Also, less polar nitroaromatics can generate more polar intermediates as a result of degradation, and the mobility in water increases with increasing polarity.[1] For example, 1,3,5-TNB is the microbiological and photochemical degradation byproduct of TNT and appears in water. The extent of hydration of nitroaromatic compounds affects the level of soil, sediment, and groundwater contamination[2−4] and can have a significant effect on industrial wastewater treatment, and in environmental risk assessment and remediation.

Measuring the properties of these very hazardous nitroaromatics is not always feasible, and it would be useful to be able to predict the properties of NACs that have not yet been synthesized. Solvent mediated reaction mechanisms and their kinetic modeling requires knowledge of the solvation free energy since the Henry's law constant, the reaction rate, and the concentration equilibrium constant are dependent on it.[5] The prediction of hydration free energies of NACs is thus important in understanding and modeling their effect on the environment, ecology, and human health.

Received: December 15, 2012
Published: May 8, 2013

Hydration free energies are of interest since chemical and environmental engineering physicochemical properties such as partition coefficients, chemical potentials, solubilities, Henry's law constants, soil sorption coefficients, and phase equilibria can be calculated from such information.[6] Also, temperature-dependent properties of NACs that are not measurable due to degradation can be calculated from the solvation free energy. In biology and drug design, the hydration free energy is an important element in understanding protein folding, biomolecular association, membrane formation, membrane transport,[7] protein−protein interactions, and ligand binding.

Most of the small molecule force fields developed for classical molecular simulations were parametrized to reproduce measured thermophysical properties (with the exception of the GROMOS 53A5 and 53A6 force fields[7] that were designed for biomolecules), and free energy calculations can be a test bed to determine their accuracy and transferability.[8−13] Many research groups have calculated solvation free energies using different estimation methods and large databases. These efforts have been important in finding weaknesses in the algorithms in sampling the entire phase space in simulations[14] and in the parametrization of force fields.[15−17] However, it has been previously found that most force fields result in predictions of limited accuracy for molecules with multiple functional groups.[9] Here, we consider the behavior of a number of available force fields for a particular class of multifunctional compounds, the NACs, with both published atomic charges and ones we compute here.

Although the history of force field (FF) development goes back to the 1950s, the introduction of parameters for nitroaromatic compounds (NACs) has been a recent development. OPLS-AA FF[18] was the first to provide parameters for NACs. Klauda and Brooks[19] introduced CHARMM FF parameters for nitroalkanes and nitroarenes (C27rn), and subsequently Vanommeslaeghe et al.[17] provided nitroaromatic parameters in CGenFF[17] (CHARMM Generalized Force Field). Parameters have been introduced in the AMBER FF for nitro groups connected to an aromatic ring in its small molecule version GAFF (Generalized AMBER Force Field).[20] The TraPPE FF[21−25] (Transferable Potentials for phase Equilibria Force Field) has gradually been improved for nitroaromatic compounds, and the most recent version includes explicit hydrogen parameters for nitrobenzene, aniline, and 1,3,5-triamino-2,4,6-trinitrobenzene (TATB).[23] However, most of the NACs of interest contain more than one nitro group and one alkyl group, and finding successful FF parameters for NACs with multiple functional groups has been challenging. Also, many of the force fields lead to results that are not very accurate for compounds containing nitro groups. Shivakumar et al.[26] found that for nitrogen-containing polar functional groups, such as amines and amides, using the OPLS 2005 parameters and charges in simulation led to solvation free energy errors of greater than 1.3 kcal/mol compared to experimental data. The earlier version of AMBER FF was also of limited accuracy for these compounds.[27] Later with GAFF/AM1-BCC FF, Mobley et al.[28] found somewhat better agreement (an average unsigned error, AUE, of 1.03 kcal/mol). Using CM1A-BCC computed charges, Shivakumar et al.[26] also found better agreement with experimental data using the OPLS 2005[29] parameters.

It has been found that charges calculated from one method (either quantum or semiempirical) that are good for certain classes of functional groups may not suitable for other functional groups.[26] By using the Poisson−Boltzmann (PB) and Generalized Born (GB) continuum methods in conjunction with the solvent-accessible surface area (SA) term, Rizzo et al.[30] found that they could not reproduce the experimental hydration free energies of nitro-containing molecules. They attributed this to the inaccuracy of the calculation methods in predicting the charge distribution. Similar difficulties in obtaining agreement with experimental data were found for nitro-containing compounds using the SGB/NP (Surface Generalized Born[31]/nonpolar) method[32] with OPLS atomic charges. Rizzo et al.[30] recommended the use of either MSK, RESP, or CHELPG partial charges obtained from quantum calculations with the 6-31G* basis set or the AM1-BCC semiempirical charges over other quantum or approximation methods.

The partial charges assigned to atoms during parametrization together with the other FF parameters have been found to provide good agreement with experimental data for some thermophysical properties.[33] Previously, quantum and semiclassical charge reassignment methods have been used and found to lead to improved solvation free energy predictions,[13,18,34,35] and this is also done here.

One of the goals of the work here is to identify an appropriate force field, water model, and charge calculation method for multifunctional nitroaromatic compounds for use in simulation. Another aspect of this work is to establish a pathway to obtain reliable solvation free energies for compounds in the absence of reported experimental data.

The number and types of functional groups have a significant effect on the solvation free energy;[13,36] however, a systematic study on the effect of multiple functional groups on the parametrization of the FF and on the charge assignment method is not available. Here we focus on the effects of the number of functional groups, the water model used, and the charge assignment method for a detailed analysis of the force fields for NACs.

This paper is organized as follows. In the following section, the essential components of the EE algorithm used here are very briefly discussed. This is followed by the details of the force field parameter assignment for a given molecular geometry, the assignment of partial charges, and the methodologies involved for these. The results are presented sequentially highlighting the effects of the water models, partial charges, and force field parameters. The similarities and contrasts of the different methods are presented in the results and discussion sections, and supplemented with literature data that answer some questions that arose.

II. SIMULATION DETAILS

A. Method of Solvation Free Energy Calculation.

Although conventional molecular simulation techniques can be used to compute solvation free energies, a significant number of independent simulations both for equilibration and production are needed, and some also require post processing to calculate the solvation free energies. In contrast, the expanded ensemble (EE) algorithm requires only a single converged production run. Efficiency and adequate conformation sampling are the key advantages of using the EE algorithm. The essential statistical mechanics background for the algorithm can be found in the earlier literature.[37−42] The details of the built-in error estimation procedure in sampling the entire phase space and the coupling parameter space can be found elsewhere.[43] All simulations here were carried out using the isothermal−isobaric (*NPT*) version of the EE algorithm with an automated

optimization scheme for the balancing factors[44] in the MDynaMix package version 5.2.4.[42,44]

B. Force Fields and Partial Atomic Charges. OPLS-AA, GAFF, CGenFF, and TraPPE force field parameters either with default (charges obtained as part of the FF development) or calculated partial atomic charges were used in the simulations. The default charges are available for the OPLS-AA and TraPPE force fields; however, the TraPPE charges for NACs were found to suffer from transferability problems to other compounds for which they were not calculated.[45] The CHELPG and RESP gas-phase charges and CM4 aqueous-phase charges were used with all the force fields studied here. Also, the semiempirical AM1-BCC charges were used with GAFF, and the charges obtained from ParamChem[46−48] were used with CGenFF to examine the suitability of these charges for nitroaromatic compounds. CHELPG[49] charges were calculated using Gaussian 09 at B3LYP/6-311G(d,p) with the optimized geometry at B3LYP/6-31G(d) and with the dipole moment preserved. The RESP charges were calculated using the R.E.D. server at the HF/6-31G* level with optimized geometry at the same level of theory and basis set.[50,51] The aqueous phase CM4 charges were calculated using SMxGauss[52,53] version 3.3 at the mPW1PW91/MIDI!6D[54] level using the SM6 continuum solvation model and the gas-phase optimized geometries obtained using Gaussian 09[55] at the B3LYP/cc-pVTZ[56] level. AM1-BCC[34,57] charges were obtained using AmberTools-1.5,[58] and the ParamChem charges were calculated using the ParamChem web server.[46−48] The details of the parameter and charge assignments for modeling the NACs used in the simulations can be found in section VI of the Supporting Information.

The TIP3P[59] water model was used with all the solute force fields studied here; however, with the CHELPG charges the SPC-Fw[60] water model was also used to determine how this model, with its flexibility, influences the solvation free energy results of CGenFF only. As the TIP3P water model has been previously used in numerous studies, it is useful here in benchmarking the solute force fields.

C. Expanded Ensemble Molecular Dynamics Simulation Conditions. All the simulations were carried at room temperature and 1 atm pressure. Each simulation consisted of 500 water molecules and a single nitroaromatic solute. In the *NPT* simulations, the temperature and pressure were regulated using the Nose-Hoover[61,62] thermostat and barostat with relaxation times of 30 and 700 fs, respectively. The Ewald[63,64] summation technique was used to calculate the Coulombic contribution to the solute−solvent interactions. Twenty subensembles were used in each of the EE simulations, and the corresponding 20 coupling parameters were uniformly spaced between the 0 (uncoupled) and 1 (fully coupled) states of the solute with the solvent molecules. The Lennard-Jones ε parameters were scaled as the fourth power of the coupling parameter. The σ parameters were scaled linearly, and the atomic charges were scaled as the square of the coupling parameter.[44,65] The balancing factors were determined using the Wang−Landau (WL) procedure that has been incorporated into the EE algorithm for their efficient optimization during the single simulation production run. The balancing factors were incremented in steps of 0.1 during optimization and scaled by 0.5 after each WL iteration. For each of the nitroaromatics, the EE simulation was run for 20 ns, of which the first 10 ns were used to optimize the balancing factors, and the remainder was used for production and to collect the statistical errors. The uncertainty in each solvation free energy was calculated using the block averaging method, and an equal number of blocks was used for all solvation free energy calculations reported here.[35,42] A simulation was rejected unless it passed through the two extreme subensembles at least several times during a single WL iteration. Also, the simulations were examined for approximately equal orders of magnitude over the probability distributions, and approximately equal forward and reverse acceptance ratios. The details for the examination of phase space sampling and overlap between neighboring subensembles implemented in the EE algorithm are given elsewhere.[43,66]

D. Calculation of the Abraham Method LSER Solvation Free Energies. The Abraham descriptors (details of the sources of descriptors can be found in section VI(B) of the Supporting Information) were used to estimate the air−water partition (K_{AW}) coefficients of the NACs using[67]

$$\log_{10} K_{AW} = -1.271 + 0.822E + 2.743S + 3.904A + 4.814B - 0.213L \quad (1)$$

and then the solvation free energies in water (ΔG_{hyd}) were calculated using[5,53,68]

$$\Delta G_{hyd} = -2.303RT \log_{10} K_{AW} \quad (2)$$

The solute descriptors A (overall hydrogen bond donating ability or acidity, which is a measure of the strength of hydrogen bonding of the solute in a basic solvent), B (overall hydrogen bond accepting ability or basicity, which is a measure of the strength of hydrogen bonding of the solute in an acidic solvent), E (excess molar refractivity, which accounts for the polarizability of the solute and quantifies the ability of a solute molecule to interact with a solvent through n-and-π electron pairs), S (measure of propensity of the solute for electrostatic interactions associated with dipolarity and polarizability effects through stabilizing charge or dipole), and L (logarithm of the gas-hexadecane partition coefficient at 298 K) can be obtained either from experimental data[53] or from prediction.[5] Table ST3 of the Supporting Information contains the Abraham descriptors for the NACs.

E. Calculation of Solvation Free Energy Using a Continuum Solvation Model. Two different sets of calculations using the SM6[69] implicit solvation model were done for the solvation free energies. In the first set of calculations, the molecular geometries were first optimized using Gaussian 09 at the B3LYP level of theory with the correlation consistent polarized triple-ζ (cc-pVTZ)[56] basis set. It has been shown that the use of B3LYP does not compromise the accuracy of the SM6 model, and the combination with B3LYP/cc-pVTZ is computationally efficient.[70] These optimized geometries were used to calculate the solvation free energies using the SM6 model with the mPW1PW91[54] hybrid DFT (Density Functional Theory) functionals of Adamo and Barone[54] and the MIDI!6D basis set. In the second set of calculations, the optimized geometries from the first set of calculations were used; however, the solvation free energies were calculated using B3LYP/6-31+G(d,p).

III. THE SOURCES OF EXPERIMENTAL SOLVATION FREE ENERGY DATA AND VALIDATION PROCEDURE

Accurate experimental data are essential for the validation of the simulation and the force field parameters used. Also, the definition of the standard state is important to ensure that the

Table 1. Hydration Free Energies (in kcal/mol) of Nitroaromatic Compounds Using CHELPG Charges and TIP3P and SPC-Fw Water Models

NAC	experiment	GAFF/(CHELPG +TIP3P)	OPLS-AA /(CHELPG+ TIP3P)	CGenFF/(CHELPG +SPC-Fw)	CGenFF/(CHELPG+ TIP3P)	TraPPE-UA/(CHELPG +TIP3P)
2-NT	−3.68 ± 0.06	−3.44 ± 0.08	−3.30 ± 0.15	−3.50 ± 0.14	−3.49 ± 0.09	−3.31 ± 0.09
3-NT	−3.45 ± 0.0	−3.66 ± 0.07	−3.39 ± 0.17	−3.65 ± 0.17	−3.62 ± 0.10	−3.37 ± 0.10
4-NT	−4.16 ± 0.58	−3.72 ± 0.07	−3.61 ± 0.14	−3.64 ± 0.18	−3.64 ± 0.07	−3.67 ± 0.08
2,3-DNT	−6.37 ± 0.11	−7.16 ± 0.08	−6.79 ± 0.26	−7.27 ± 0.22	−7.21 ± 0.10	−5.64 ± 0.10
2,4-DNT	−6.77 ± 0.14	−7.80 ± 0.09	−7.29 ± 0.15	−7.36 ± 0.16	−7.11 ± 0.09	−7.14 ± 0.08
2,6-DNT	−6.14 ± 0.10	−7.61 ± 0.06	−7.48 ± 0.28	−7.04 ± 0.17	−7.03 ± 0.07	−6.83 ± 0.08
3,4-DNT	−6.75 ± 0.17	−7.40 ± 0.07	−6.69 ± 0.23	−7.09 ± 0.18	−7.29 ± 0.09	−5.46 ± 0.07
2,4,6-TNT	−8.43 ± 0.27	−11.00 ± 0.09	−10.31 ± 0.21	−9.85 ± 0.21	−9.52 ± 0.11	−9.85 ± 0.09
1,3,5-TNB	−9.49 ± 0.22	−11.65 ± 0.07	−10.37 ± 0.17	−10.04 ± 0.22	−9.93 ± 0.10	−9.47 ± 0.13
AUE		**1.06**	**0.68**	**0.62**	**0.56**	**0.61**

Table 4. Hydration Free Energies (in kcal/mol) of Nitroaromatic Compounds Using CM4 Charges and TIP3P Water Model

NAC	experiment	GAFF/(CM4+TIP3P)	OPLS-AA /(CM4+ TIP3P)	CGenFF/(CM4 + TIP3P)	TraPPE-UA/(CM4 +TIP3P)
2-NT	−3.68 ± 0.06	−3.59 ± 0.07	−3.32 ± 0.06	−3.32 ± 0.05	−2.89 ± 0.07
3-NT	−3.45 ± 0.0	−3.92 ± 0.04	−3.64 ± 0.07	−3.71 ± 0.05	−3.17 ± 0.08
4-NT	−4.16 ± 0.58	−4.28 ± 0.05	−3.83 ± 0.07	−3.92 ± 0.09	−3.63 ± 0.05
2,3-DNT	−6.37 ± 0.11	−8.90 ± 0.06	−8.12 ± 0.06	−7.77 ± 0.09	−6.76 ± 0.09
2,4-DNT	−6.77 ± 0.14	−7.98 ± 0.05	−7.35 ± 0.08	−6.92 ± 0.07	−6.74 ± 0.08
2,6-DNT	−6.14 ± 0.10	−6.92 ± 0.07	−6.32 ± 0.07	−5.95 ± 0.08	−5.44 ± 0.07
3,4-DNT	−6.75 ± 0.17	−9.64 ± 0.09	−9.03 ± 0.09	−8.69 ± 0.07	−7.16 ± 0.07
2,4,6-TNT	−8.43 ± 0.27	−10.27 ± 0.08	−8.64 ± 0.08	−8.01 ± 0.10	−7.66 ± 0.07
1,3,5-TNB	−9.49 ± 0.22	−11.96 ± 0.08	−10.07 ± 0.08	−9.52 ± 0.12	−8.18 ± 0.07
AUE		**1.38**	**0.72**	**0.56**	**0.58**

simulation corresponds to the experimental data.[5] The solvation free energy standard state definition of Ben-Naim and Marcus[71] is widely accepted, although other definitions are also equally valid and interconvertible.[72] Here, we report all solvation free energy data using the Ben-Naim standard state.

As solvation free energies cannot be measured directly, there are several methods for their calculation from other measurements.[68,71,73] The most common experimental method of determining solvation free energies is from the measured ratio of the molar concentrations of the solute in its pure gas to that in a solvent liquid phase at a specified composition.[73,74] The experimental solvation free energy database compiled by Katritzky et al.[73,75] is one of the largest, with data for approximately 500 compounds in 69 solvents; other smaller databases are by Rizzo et al.[30] and by Ben-Naim and Marcus,[71] all using the same standard state definition.

To compute the solvation free energy of a compound that is not in the existing databases, the methods of Marenich et al.[68] can be used when vapor pressure data, solubility, and the Henry's law constant in water (or the air/water partition coefficient) are available. If vapor pressure data are not available at the temperature of interest, interpolation/extrapolation methods can be used.

Here we briefly summarize the methods that we have used for calculating solvation free energies from experimental data. Following Marenich et al.,[68] the solvation free energy is calculated either from solubility in molarity units (S_{aq}) and vapor pressure (P_{vap}) data or from dimensionless Henry's law constant (H_{dl}) using the following equations:

$$\Delta G_{hyd} = -2.303RT \log_{10}\left(\frac{S_{aq}/M^0}{P_{vap}/P^0}\right) \quad (3)$$

and

$$\Delta G_{hyd} = 2.303RT \log_{10} H_{dl} \quad (4)$$

where M^0 = 1 mol/L and P^0 = 24.45 atm of pressure of an ideal gas (resulting in a 1 molar concentration at 298 K). Rizzo et al.[30] reported solvation free energies of 500 neutral and charged compounds calculated from the air/water partition coefficients (eq 2) collected from Bordner et al.[76] and also by using the Abraham solute descriptor method (eq 1). Ben-Naim and Marcus calculated solvation and self-solvation free energies for a number of compounds using saturated vapor pressure, liquid density, and the temperature coefficients of a liquid phase density correlation.[71]

The calculated solvation free energies using different methods vary depending on the quality and variations of the experimental data. The very low vapor pressures of sparingly soluble NACs make measurements difficult, and there are considerable discrepancies in the values reported in the literature.[77] To mitigate this problem, we have calculated solvation free energies from available experimental data using different methods and estimated the standard deviations. The extreme outliers (typically several kcal/mol) from the general trends of the experimental data were ignored. Also the NACs studied here, except for 2- and 3-nitrotoluene, are solids at room temperature.

We have calculated solvation free energies from available solubility and vapor pressure data using available sublimation pressures at room temperature of the solid compounds. The

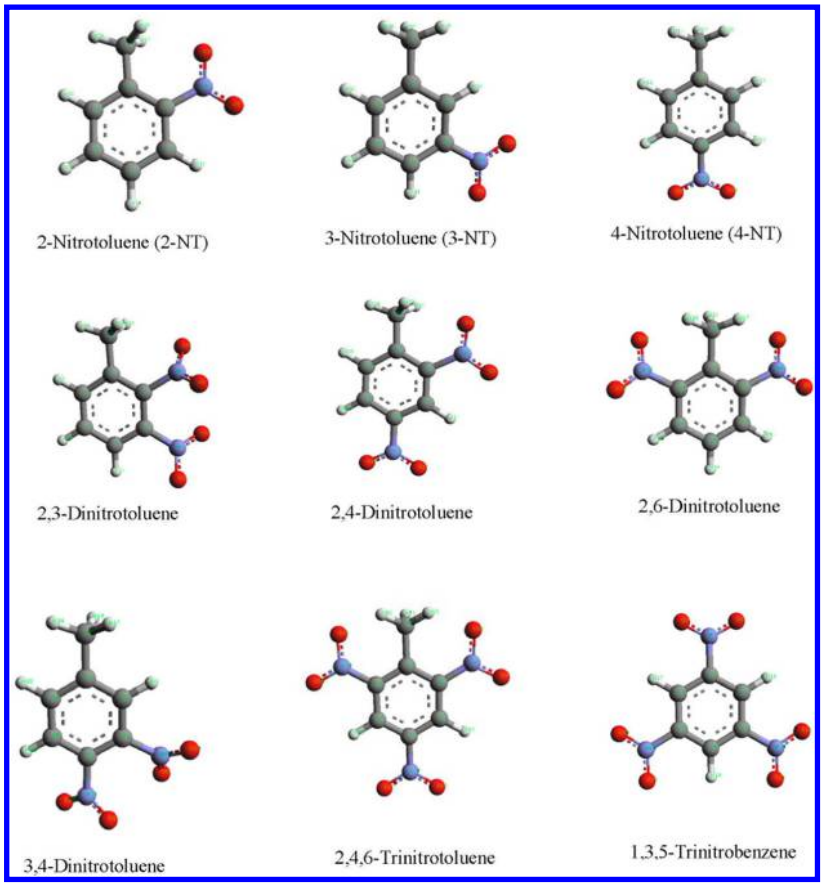

Figure 1. Molecular structures of the nitroaromatic compounds (NACs) studied here.

calculated values and the details of the solubility, vapor pressure, and Henry's law constant data, including their sources, are compiled in Tables ST6−ST21 of the SI. The experimental solvation free energy data for the NACs are summarized in Table ST2 of the SI and also reported in Tables 1−4.

For 2-NT, the solvation free energy in water calculated from the measured Henry's law constant was found to be underestimated by 0.81 kcal/mol compared to that calculated from experimental solubility and vapor pressure data. Since there are nine solvation free energies for 2-NT calculated from available experimental solubility and vapor pressure data with a standard deviation of only 0.06 kcal/mol, the solvation free energy calculated from the Henry's law constant was ignored in Table ST2 of the SI. We also compared our 2-NT hydration free energy data with that reported by Abraham et al.[53] and adopted in two recent databases,[28,30] and the difference was only 0.1 kcal/mol.

For 3-NT, the calculated solvation free energy from the experimental Henry's law data was 1.22 kcal/mol lower than that calculated from the measured solubility and vapor pressure data. Since the reported data for 3-NT are close to that calculated from the solubility and vapor pressure data, the Henry's law constant data were ignored here as well. The experimental data for 3-NT reported by Abraham et al.[53] was identical to that obtained from the measured solubility and vapor pressure data. They reported measured air−water partition coefficient data, and the hydration free energy was calculated using eq 2.

For 2,4-DNT, the solvation free energy calculated from the experimental Henry's law constant was 0.96 kcal less than that calculated from experimental solubility and vapor pressure data. Since 24 calculated solvation free energies using different combinations of solubility and vapor pressure were all within the standard deviation of 0.14 kcal/mol, the result based on the Henry's law constant was not considered in averaging. Our calculated solvation free energy data of 1,3,5-TNB is different from that previously reported by Kelly et al.[78] using the solubility and vapor pressure data of Walsh et al.,[79] though in their calculations they used solubility and vapor pressure data at 20 °C, while our calculations use the room temperature data.

Since generally the solubility and vapor pressure measurements are done by different investigators, we have calculated the solvation free energy for all combinations of available vapor pressure and solubility data, and only those data were accepted that follow the main trend, with the extreme outliers being excluded. For well-studied small molecules such as amino acid side chain analogs, Shirts and Pande[80] found that experimental data vary between 0.03 and 0.07 kcal/mol; for most of the NACs, solvation free energies calculated from the experimental data varied between 0.07 and 0.27 kcal/mol. However, for 4-NT hydration, free energy calculated from the experimental data varies up to 0.58 kcal/mol due to significant variations in the reported vapor pressure and solubility data. The zero standard deviation we report for 3-NT is due to the scarcity of available experimental data.

Table 2. Hydration Free Energies (in kcal/mol) of Nitroaromatic Compounds Using TIP3P Water Model and Force-Field Specific Default Charges, AM1-BCC Charges with GAFF, Abraham LSER Method, and SM6 Implicit Solvation Model

						SM6 implicit solvation model	
NAC	experiment	GAFF/(AM1-BCC + TIP3P)	OPLS-AA/(Default Charge+TIP3P)	CGenFF/(ParamChem Charge+TIP3P)	Abraham LSER method	mPW1PW91/ MIDI!6D	B3LYP/6-31+G(d, p)
2-NT	−3.68 ± 0.06	−3.28 ± 0.07	−2.28 ± 0.23	−3.11 ± 0.15	−3.88	−3.33	−4.65
3-NT	−3.45 ± 0.0	−2.72 ± 0.06	−2.30 ± 0.30	−3.30 ± 0.16	−3.65	−3.76	−4.81
4-NT	−4.16 ± 0.58	−2.97 ± 0.07	−2.59 ± 0.13	−3.17 ± 0.13	−3.88	−3.97	−5.12
2,3-DNT	−6.37 ± 0.11	−4.95 ± 0.06	−5.17 ± 0.17	−7.99 ± 0.15	−6.98	−6.72	−7.72
2,4-DNT	−6.77 ± 0.14	−4.61 ± 0.05	−5.91 ± 0.17	−7.96 ± 0.17	−7.08	−6.08	−7.00
2,6-DNT	−6.14 ± 0.10	−4.59 ± 0.07	−5.38 ± 0.12	−8.08 ± 0.21	−6.78	−5.55	−5.65
3,4-DNT	−6.75 ± 0.17	−4.97 ± 0.07	−5.25 ± 0.16	−8.23 ± 0.17	−6.42	−7.42	−8.07
2,4,6-TNT	−8.43 ± 0.27	−5.24 ± 0.08	−9.95 ± 0.22	−13.46 ± 0.16	−10.11	−7.65	−6.37
1,3,5-TNB	−9.49 ± 0.22	−5.24 ± 0.07	−10.76 ± 0.14	−14.22 ± 0.25	−10.52	−8.96	−6.57
AUE		**1.85**	**1.25**	**1.97**	**0.59**	**0.50**	**1.29**

Table 3. Hydration Free Energies (in kcal/mol) of Nitroaromatic Compounds Using RESP Charges and TIP3P Water Model

NAC	experiment	GAFF/(RESP+TIP3P)	OPLS-AA /(RESP+ TIP3P)	CGenFF/(RESP + TIP3P)	TraPPE-UA/(RESP +TIP3P)
2-NT	−3.68 ± 0.06	−5.65 ± 0.11	−5.32 ± 0.10	−5.36 ± 0.12	−4.68 ± 0.10
3-NT	−3.45 ± 0.0	−4.98 ± 0.08	−4.66 ± 0.13	−4.88 ± 0.10	−4.32 ± 0.10
4-NT	−4.16 ± 0.58	−5.35 ± 0.09	−4.92 ± 0.09	−5.03 ± 0.09	−4.51 ± 0.10
2,3-DNT	−6.37 ± 0.11	−9.14 ± 0.11	−8.36 ± 0.10	−8.74 ± 0.12	−6.61 ± 0.11
2,4-DNT	−6.77 ± 0.14	−9.85 ± 0.11	−9.17 ± 0.12	−8.92 ± 0.11	−9.18 ± 0.10
2,6-DNT	−6.14 ± 0.10	−9.91 ± 0.12	−9.15 ± 0.10	−8.71 ± 0.12	−8.73 ± 0.10
3,4-DNT	−6.75 ± 0.17	−9.45 ± 0.10	−8.82 ± 0.09	−9.26 ± 0.11	−6.83 ± 0.11
2,4,6-TNT	−8.43 ± 0.27	−14.14 ± 0.11	−12.74 ± 0.10	−12.13 ± 0.11	−12.83 ± 0.15
1,3,5-TNB	−9.49 ± 0.22	−15.07 ± 0.09	−13.20 ± 0.16	−12.70 ± 0.12	−12.85 ± 0.13
AUE		**3.15**	**2.34**	**2.28**	**1.70**

IV. RESULTS

A. General Performance Analyses for Force-Field/(Charge + Water) Models. *Overall Performance Analyses of Force Fields.* The computed hydration free energies for nine multifunctional nitroaromatic compounds (Figure 1) using four force fields, three charge models, default charges (whenever available with the force field), and water models are summarized in Tables 1−4. Note that the hydration free energies increase in magnitude with the number of nitro groups. Table ST4 of the SI shows the AUE (Average Unsigned) and RMSE (Root-Mean-Square) errors of the simulation results compared to the experimental data. The experimental hydration free energy data of the NACs and the simulation data obtained for all force-field/(charge + water) models in Tables 1−4 were correlated using the relationship ΔG_{sim} = (slope) × ΔG_{expt} + intercept. The trends of all the data fits are shown in Figure 2 relative to the perfect correlation (dashed) line. The correlation coefficient (R^2), the intercept, and the slope of each fit in Figure 2 are presented in Table ST4 of the SI.

Figure 2 shows that most of the experimental−simulation correlation trends depart somewhat from the experimental data with increasing negative hydration free energies, which indicates that the prediction of hydration free energies deteriorates with an increase in the number of nitro groups. For compounds with more than a single nitro group, most of the force-field/(charge+water) models predict too negative hydration free energies compared to the experimental data. However, the GAFF/(AM1-BCC+TIP3P) model always predicts more positive hydration free energies. The possible causes of such behavior will be discussed later.

The AUEs of the computed hydration free energies summarized in Table ST4 of the SI are also shown in Figure 3. The AUEs and RMSEs of all the force-field/(charge + water) models for 1, −2, and −3 nitro groups are summarized in Table ST5 of the SI; only the AUEs are shown in Figures 4−6. Since the average standard error in our collected experimental data is 0.18 kcal/mol and the standard deviations of most our simulation data are less than 0.1 kcal/mol, we consider a difference of 0.2 kcal/mol as equivalent accuracy. A comparison of the AUEs suggests that for the set of NACs studied here, 6 of 16 models perform equally well in predicting experimental hydration free energies; these are CGenFF/(CHELPG +TIP3P), CGenFF/(CM4+TIP3P), OPLS-AA/(CHELPG +TIP3P), OPLS-AA/(CM4+TIP3P), TraPPE-UA/(CHELPG +TIP3P), and TraPPE-UA/(CM4+TIP3P). Also, the flexibility of water does not have a significant effect on the hydration free energy computations, as can be seen from the comparison of the AUEs of CGenFF/(CHELPG+TIP3P) and CGenFF/(CHELPG+SPC-Fw) models.

Performance Analyses of Force Fields for Mononitro Compounds. For compounds with a single nitro group of the 16 models studied here, the hydration free energy predictabilities of all but the TraPPE force field with CHELPG and CM4 charges are close to the experimental data. The results of

dx.doi.org/10.1021/ct3011002 | J. Chem. Theory Comput. 2013, 9, 2774−2785

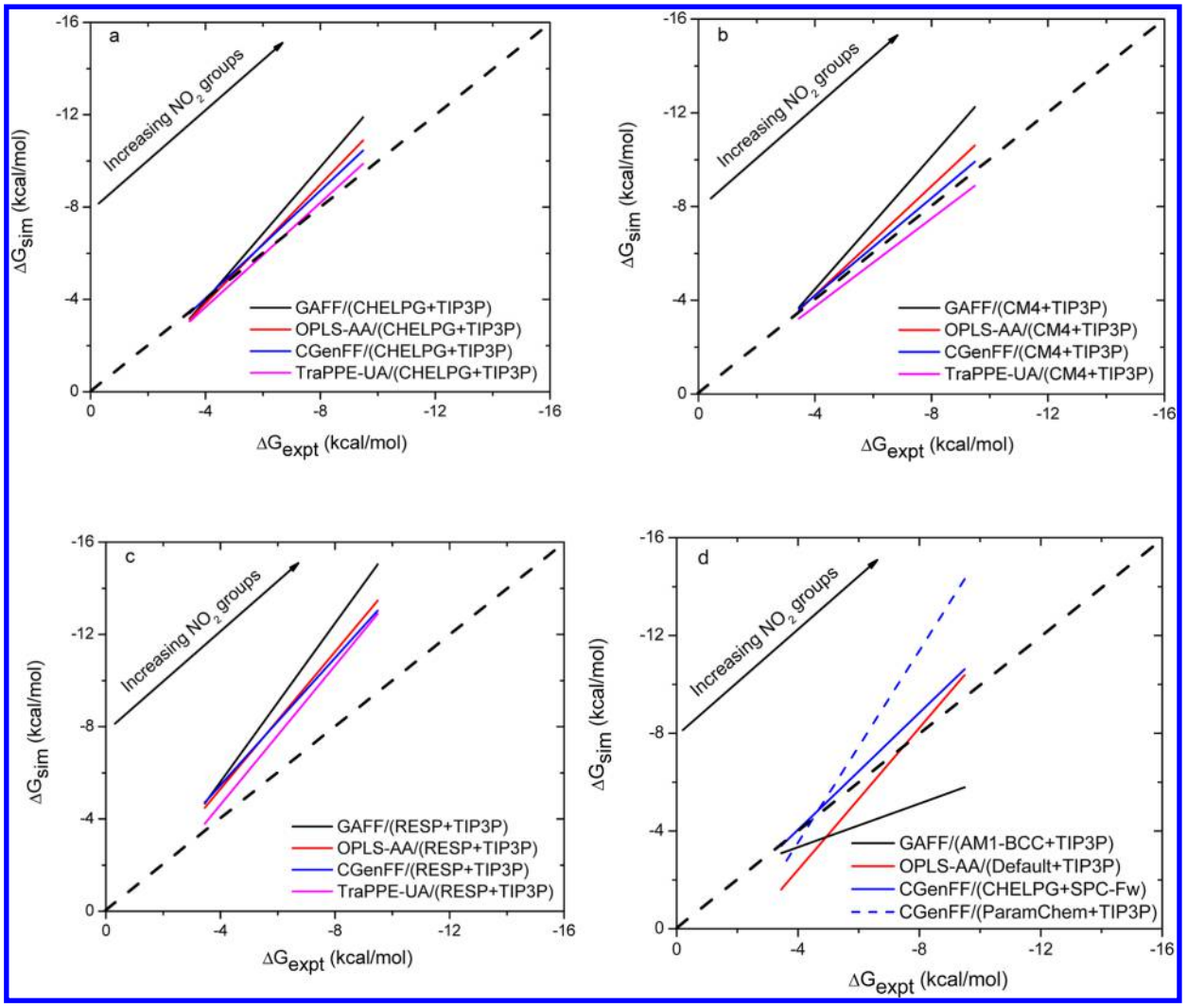

Figure 2. Trend lines of simulation data relative to experimental data. The black dashed line in each of the plots indicates perfect correlation with data, while the other lines show the deviations of the model predictions from perfect correlation. The same force field color code is used in each of the plots. The plots show the correlations between simulation results and experimental data where simulations were conducted with partial atomic charges calculated using (a) CHELPG, (b) CM4, (c) RESP, and (d) semiempirical methods. Also included are calculations using default charges and the SPC-Fw water model.

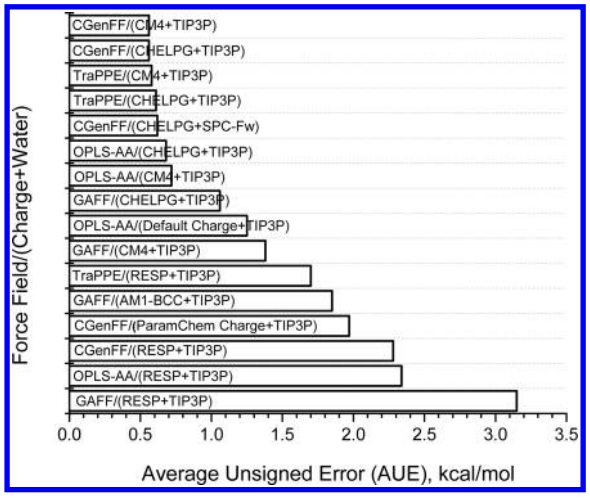

Figure 3. Performance of the force fields in reproducing experimental hydration free energies of all the NACs.

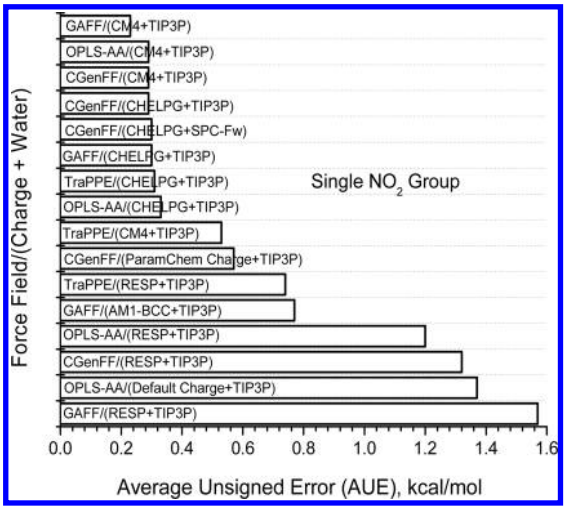

Figure 4. Performance of the force fields for single nitro group compounds in the NACs.

dx.doi.org/10.1021/ct3011002 | J. Chem. Theory Comput. 2013, 9, 2774−2785

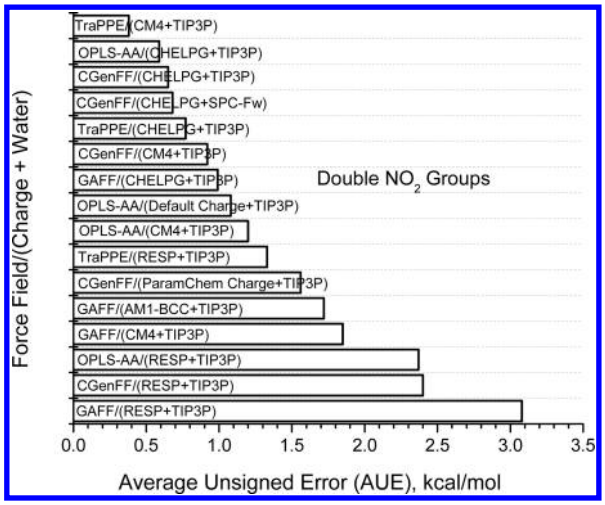

Figure 5. Performance of the force fields for dinitro group compounds in the NACs.

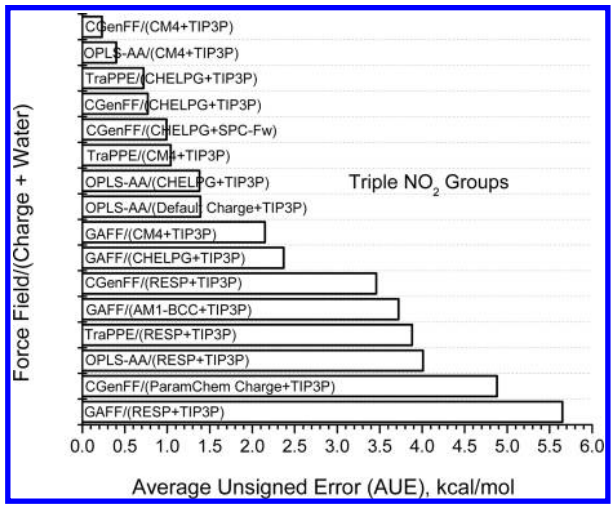

Figure 6. Performance of the force fields for trinitro group compounds in the NACs.

all the force fields using the RESP charges and the OPLS-AA/(Default-charge+TIP3P) model are the least accurate.

Performance Analyses of Force Fields for Dinitro Compounds. For two nitro-group-containing compounds, TraPPE/(CM4+TIP3P) is clearly the best in reproducing experimental hydration free energies. All but the GAFF force field with CHELPG charges perform equally well in predicting experimental hydration free energies. Also, the hydration free energies of the dinitrotoluenes predicted with CHELPG charges are approximately a factor of 2 larger than for the single nitroaromatics. The predictions of all the force fields with RESP charges are somewhat less accurate than with CM4 charges. All other models lead to AUEs of more than 1 kcal/mol, with the maximum outliers being the GAFF/(RESP+TIP3P) model.

Performance Analyses of Force Fields for Trinitro Compounds. For trinitro compounds, the CGenFF/(CM4+TIP3P) and OPLS-AA/(CM4+TIP3P) models are best in reproducing experimental hydration free energies, followed by the TraPPE/(CHELPG+TIP3P) and CGenFF/(CHELPG+TIP3P) models. Interestingly, the accuracy of the OPLS-AA/(Default-charge+TIP3P) and OPLS-AA/(CHELPG+TIP3P) models are approximately the same; that is the use of the CHELPG charges did not improve the predictions. For trinitro containing NACs, all other models have large errors, up to 5.65 kcal/mol, indicating they do not properly capture the solute/solvent interactions. In particular, the GAFF/(RESP+TIP3P), CGenFF/(ParamChem+TIP3P), and GAFF/(AM1-BCC+TIP3P) models lead to a significant increase in the errors with increasing number of nitro groups reflecting the limitation of the RESP, ParamChem, and semiempirical AM1-BCC charges compared to the CM4 and CHELPG charges in dealing with multiple nitro groups in the compound.

B. Effect of Partial Charges. It is interesting to note that the quality of the predictions of the OPLS-AA/(Default-charge+TIP3P) model does not vary significantly with increasing number of nitro groups, though they are slightly better for 2-nitro containing compounds than for 1-and 3-nitro containing compounds. The CHELPG charges for *ipso* carbons connecting methyl and nitro functional groups and exocyclic carbon in the methyl group are different from the default OPLS-AA charges. Price and Brooks[29] have previously shown how the charges in the *ipso* and exocyclic carbon of the methyl group affected the computed hydration free energy. This suggests that the default charges in the OPLS-AA FF can be improved, particularly for the NACs.

We have examined the performance of the AM1-BCC, CHELPG, RESP, and CM4 charges with the GAFF force field. The overall accuracy of the GAFF/(CHELPG+TIP3P) model is clearly better than the others followed by GAFF/(CM4+TIP3P). The predictions of the GAFF/(RESP+TIP3P) models are the least accurate with an AUE of 3.15 kcal/mol. This indicates that CHELPG or CM4 charges should be used rather than AM1-BCC or RESP charges with the GAFF FF for NACs.

C. Comparison of Force Fields with the Same Water model and the Same Set of Charges. To obtain a fair comparison of the performance of the force fields, the same water model and charge set were used. Since the solvation free energy is based on the solvent−solute interaction, the accuracy of solvation free energy predictions can be used as a tool for parameter validation.[80] Here we are comparing the latest versions of the small molecule parameter sets of two biomolecular force fields, GAFF (extension of AMBER) and CGenFF (extension of CHARMM), and two widely used force fields for liquid simulations, OPLS-AA and TraPPE-UA.

Force Fields with CHELPG Charges and TIP3P Water. Except for GAFF, all other force fields perform equally well in reproducing experimental hydration free energies of the NACs considered here. Though for single nitro group NACs, GAFF performs equally well compared to CGenFF and TraPPE-UA but distinctly less well for multiple nitro group compounds. The overall best performance of CGenFF was a result of its ability to consistently reproduce the experimental solvation free energies of mono-, di-, and trinitro group compounds. That the TraPPE-UA FF performs well is not surprising since it has been parametrized for phase equilibria. For the dinitro toluenes, except for the GAFF, the solvation free energies calculated from all the force fields with the TIP3P water and CHELPG charges combination reproduce experimental solvation free energies acceptably, but with roughly twice the AUE of single nitro-group compounds. For NACs with three nitro groups, the TraPPE-UA and the CGenFF predict experimental solvation free energies equally well with AUEs of only twice that of

dx.doi.org/10.1021/ct3011002 | J. Chem. Theory Comput. 2013, 9, 2774−2785

NACs with a single nitro group, and there are larger errors for all the other force fields.

Force Fields with CM4 Charges and TIP3P Water. Except for GAFF, all the other force fields show similar accuracy in reproducing experimental hydration free energies. For single nitro-group compounds, all but the TraPPE force fields perform equally well, though the TraPPE and CGenFF models are clearly superior in predicting hydration free energies for dinitro and trinitro NACs. The overall poor performance of the GAFF is due to the increase of the AUEs with the increasing number of nitro groups.

Force Fields with RESP Charges and TIP3P Water. The predictability of the TraPPE FF with RESP atomic charges is much better than the other force fields. The performance of TraPPE FF is consistent across all the NACs, though for trinitro-group compounds the predictability of CGenFF is slightly better. Overall, the CGenFF and OPLS-AA force fields perform equally well, but not as good as TraPPE. GAFF is the least accurate, and its AUEs increase with the number of functional groups.

D. Solvation Free Energies from the Abraham LSER Method and SM6 Solvation Model. Table 2 shows the solvation free energies predicted using the Abraham descriptor-based LSER method. The AUE of NACs solvation free energies obtained from LSER is 0.59 kcal/mol with the largest error for 2,4,6-TNT and the deviations from experimental data increase with the number of nitro groups in the compound. Overall, the Abraham LSER consistently predicts slightly too negative solvation free energies for the NACs.

The AUE of the solvation free energies (Table 2) for the NACs obtained from the SM6 continuum solvation model at mPW1PW91/MID!6D is 0.50 kcal/mol, and its performance is consistent over the number of functional groups. However, the solvation free energies calculated using B3LYP/6-31+G(d,p) differ significantly from the experimental data with an AUE of 1.29 kcal/mol, and the predictions are worst for 3-nitro-containing compounds.

V. DISCUSSION

A. Trends in Experimental Hydration Free Energy Data: What is the Effect of the Nitro Groups? The experimental data in Tables 1−4 (also summarized in Table ST2 of the SI with the data sources) suggest that the number of nitro groups in the nitroaromatics studied and their relative positions on the aromatic ring determine the magnitude of the hydration free energy, and presumably the hydration structure around the solute. The hydration free energy monotonically increases in magnitude with the number of nitro groups. Comparison of the solvation free energies of single and dinitro toluenes indicates that solvation free energies are not additive with the number of nitro groups in the aromatic ring. Also, the spatial positions of the functional groups are important, as suggested by Fennell and Dill.[81] The relative position of the nitro groups to one another and to the methyl group is also important in determining the solvation free energy, as are the solvent accessible surface area (or volume) and surface curvature.[81] Also, a comparison of the solvation free energies indicates that the presence of a methyl group in 2,4,6-TNT makes it more hydrophobic than 1,3,5-TNB in which the methyl group is absent.

B. Comparison with Previous Work. There are number of databases[26,28,30] of hydration free energies available in the literature, and most consider only small and drug-like molecules, because of the availability of accurate experimental data and the industrial importance of those compounds. Here we have calculated the solvation free energies for environmentally important NACs for which only limited experimental data are available.

Shivakumar et al.[82] included seven nitro compounds in their test set, of which only three are nitroaromatic compounds. For these nitro containing compounds they used the GAFF/(RESP+TIP3P), GAFF/(CHELPG+TIP3P), GAFF/(AM1+TIP3P), CHARMm-MSI/(CHELPG+TIP3P), and CHARMm-MSI/(AM1+TIP3P) force fields to calculate hydration free energies. For all the nitro compounds they considered, including 2-NT, they found that the CHARMm-MSI/(AM1-BCC+TIP3P) model was the best. The absolute deviations of their simulation results for 2-NT using GAFF/(RESP+TIP3P) and GAFF/(CHELPG+TIP3P) were 1.98 and 1 kcal/mol, respectively. However, for nitroaromatic compounds with only a single nitro group, GAFF/(CHELPG+TIP3P) was the best with an AUE of 0.86 kcal/mol, in agreement with our findings for similar compounds. Mobley et al.[28] included 17 nitro compounds in their test set, of which 11 were nitroaromatics. The AUE was 1.04 kcal/mol for the nitroaromatics. For 2-NT and 3-NT, their AUE was 0.42 kcal/mol compared to our value of 0.56 kcal/mol when GAFF/(AM1-BCC+TIP3P) was used.

C. An Assessment of Charge Models. In many hydration free energy simulation studies, the AM1-BCC charges were found to lead predictions of comparable accuracy to those using more rigorous DFT methods for molecules with different functionality.[13] It is interesting to note that Shivakumar et al.[82] found that the AM1-BCC method outperformed RESP charges for compounds with nitrogen-containing polar functional groups. In particular for 2-NT, the absolute errors of their predictions using RESP and AM1-BCC were 1.98 and 1.22 kcal/mol, respectively, whereas our computations lead to absolute errors of 1.97 and 0.4 kcal/mol. For the NACs studied here, the predictions of GAFF with AM1-BCC charges are clearly better than with RESP charges.

In the calculations here for NACs with more than one nitro group, the AM1-BCC charges result in hydration free energies that are too positive compared to the experimental data. Since using the same set of GAFF parameters, but with CHELPG and CM4 charges, results in better hydration free energies, the AM1-BCC charges are responsible for poorer predictions. A similar overprediction of solvation free energies was also found by Shivkumar et al.[82] for nitriles and alkynes. Further, Nicholls et al.[10] found that the predicted solvation free energies for esters, benzamides, and imidazole with the GAFF parameters using AM1-BCC v1, AM1-BCC v2.6A24, and RESP charges were all of only limited accuracy. Thus, we conclude that AM1-BCC charges should not be used for the NACs.

D. How Well Do the Force Fields Represent NACs? Since Mobley et al.[28] calculated the solvation free energies of 2-NT and 3-NT using GAFF/(AM1-BCC+TIP3P) it is interesting to compare our results with theirs. Our prediction for single nitro-group compounds using GAFF/(AM1-BCC+TIP3P) differs on average by 0.14 kcal/mol from the results of Mobley et al.[28] Considering the differences in integration schemes, thermostats, the scaling of Lennard-Jones parameters, and the treatment of the electrostatic interactions in the GROMACS (used by Mobley et al.) and MDynaMix (used here) simulation packages, the agreement is within the standard deviations of these methods. Also, this difference is within the average standard deviations of the experimental data of NACs.

Shirts and Pande[80] observed similar differences compared to the results of Maccallum and Tieleman[83] and also attributed this difference to the simulation methods.

Shivakumar et al.[82] also computed the solvation free energy of 2-NT using a combination of the explicit TIP3P water model and implicit spherical solvent boundary potential (SSBP) for simulating compounds with the GAFF parameters and CHELPG charges and found a value of −4.68 kcal/mol, which differs by 1.0 kcal/mol from the experimental data. In contrast, the hydration free energy result for 2-NT we obtained using GAFF/(TIP3P+CHELPG) differs by only 0.24 kcal/mol from the experimental data; the difference between the results of Shivakumar et al. and ours can partially be attributed to their implicit treatment of the solvent.

Caleman et al.[33] found that using GAFF for nitro-group-containing compounds leads to predictions of higher densities and enthalpies of vaporization than experiment, which they attributed to the high nitro group charges in the model. Our study indicates that it is not only the charges but also the FF parameters that are responsible for this. Recently Boyer and Bryan[84] argued that the GAFF oxygen (O) atom type in the nitro group poorly accounts for the chemical environment since in GAFF the resonant bond structure of an oxygen atom connected to a nitrogen atom is represented by only a single bond. To analyze this we examined the nitro group force field parameters for the different force fields considered here. It is clear from Figure 7a that the Lennard-Jones (LJ) σ parameters for the nitrogen and oxygen atoms are approximately the same for all force fields studied here, but the LJ ϵ parameters are significantly different. By changing the LJ water oxygen ϵ parameter from 0.1521 to 0.25 kcal/mol and using the TIP3P water model, Shirts and Pande[80] demonstrated that for amino acid side chains the solvation free energies in water can be improved by an average of −0.50 kcal/mol without affecting the liquid water properties. Figure 7b suggests that the differences of the nitro group atoms (N and O) LJ ϵ parameters in the different force fields is in part responsible for the different hydration free energies obtained from simulations. Price and Brooks[29] demonstrated that the change in LJ well depth improves the hydration free energy of nitrobenzene relative to benzene.

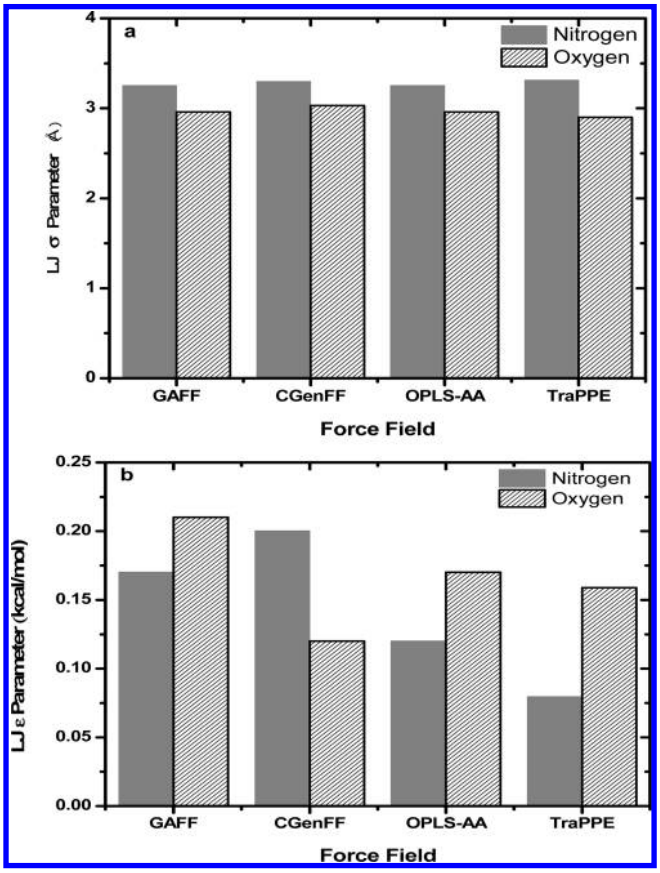

Figure 7. Comparison of the Lennard-Jones (a) σ (atomic diameter) and (b) ϵ (potential well depth) parameters of nitro group nitrogen and oxygen atom for different force fields.

VI. CONCLUSIONS

Expanded ensemble molecular dynamics simulations were carried out for nine nitroaromatic compounds using the TIP3P water model with the GAFF, CGenFF, OPLS-AA, and TraPPE force fields. The CHELPG, RESP, and CM4 charges were used for all these force fields. Also AM1-BCC charges were used with GAFF, and the default charges of the OPLS-AA FF were used.

With all the force fields the CHELPG and CM4 charges led to better predictions than either the default, the RESP, or the AM1-BCC charges. The predictabilities of the CGenFF/(CHELPG+TIP3P), CGenFF/(CM4+TIP3P), OPLS-AA/(CHELPG+TIP3P), OPLS-AA/(CM4+TIP3P), TraPPE-UA/(CHELPG+TIP3P), and TraPPE-UA/(CM4+TIP3P) models are found to be of similar quality for the 16 force field charge models we studied. With all charge models the accuracy of the hydration free energy predictions using GAFF parameters decreased with increasing number of nitro groups in the compounds. Also, the flexibility of water did not improve the predictions of NACs solvation free energies.

Our study suggests that van der Waals parameters of nitro group atoms in the force fields are responsible for the variation of predicted hydration free energies of the NACs even with the same combination of charge and water models. This observation suggests a reparameterization is needed of the nitro group parameters when there are multiple nitro groups in a compound.

We also analyzed the performance of the simulation-based methods compared to the Abraham LSER method for the prediction of solvation free energies. We found that the predictions of the Abraham method are comparable to the best force field although the error increases with an increasing number of nitro groups in the NACs. The unavailability of experimental descriptors is partially responsible for this, and the calculation of descriptors using the Platts fragment method is reasonable for the NACs studied here.

We also compared the performance of the method here with that of the SM6 continuum solvation model. SM6 solvation free energy calculations at mPW1PW91/MIDI!6D perform equally well to the best force fields used here in the EE simulations; however, calculations at B3LYP/6-31+G(d,p) are worse than the methods here. For both sets of calculations, B3LYP/cc-pVTZ optimized geometries were used. Although SM6 solvation model calculations are faster than the force-field-based simulations, a definitive conclusion as to its use cannot be made because of the numerous choices of DFT theory levels and basis sets that can be used, and it is not known in advance which lead to acceptable predictions.

Another conclusion of this work is that for the multifunctional compounds of practical interest, of which the NACs considered here are an example, there is room for improvement of all the force fields discussed.

■ ASSOCIATED CONTENT

Supporting Information

Figures SF1−SF4: molecular structures of NACs (SF1) and fitting of solubility data (SF2−SF4). Tables ST1−ST23: molecular information of NACs (ST1), experimental hydration free energies of NACs (ST2), Abraham LSER descriptors of NACs (ST3), overall statistics of computed hydration free energies compared to experimental data (ST4), AUEs and RMSEs grouped based on the number of nitro groups in the NACs (ST5), calculation of experimental hydration free energies from measured vapor pressure, solubility, and Henry's law constant data (ST6−ST21), and CHELPG and CM4 partial atomic charges for 3,4-DNT (ST22) and 2,4,6 TNT (ST23). This material is available free of charge via the Internet at http://pubs.acs.org.

■ AUTHOR INFORMATION

Corresponding Author

*Phone: 302-831-2945. Fax: 302-831-8201. E-mail: sandler@udel.edu.

Notes

The authors declare no competing financial interest.

■ ACKNOWLEDGMENTS

This work has been supported by National Science Foundation (NSF) grant GOALI-0853685 and the Strategic Environmental Research and Development Program (SERDP) grant ER-1734. This work used the Extreme Science and Engineering Discovery Environment (XSEDE), which is supported by National Science Foundation grant number OCI-1053575. A.A. acknowledges the discussions with Prof. J. Ilja Siepmann, Prof. Alex MacKerell, and Dr. Kenno Vanommeslaeghe.

■ REFERENCES

(1) Schmidt, A.-C.; Niehus, B.; Matysik, F.-M.; Engewald, W. *Chromatographia* **2006**, *63*, 1−11.
(2) Roberts, M. G.; Rugh, C. L.; Li, H.; Teppen, B. J.; Boyd, S. A. *Environ. Sci. Technol.* **2007**, *41*, 1641−1645.
(3) Walsh, M. E.; Ranney, T. A. *Determination of nitroaromatic, nitramine, and nitrate ester explosives in water using SPE and GC/ECD; comparison with HPLC*; Special Report 98−2, U.S. Army Cold Regions Research and Engineering Laboratory: Hanover, NH, 1998.
(4) Zhang, D.; Zhu, D.; Chen, W. *Environ. Toxicol. Chem.* **2009**, *28*, 1447−1454.
(5) Jalan, A.; Ashcraft, R. W.; West, R. H.; Green, W. H. *Annu. Rep. Prog. Chem., Sect. C: Phys. Chem.* **2010**, *106*, 211−258.
(6) Thompson, J. D.; Cramer, C. J.; Truhlar, D. G. *J. Chem. Phys.* **2003**, *119*, 1661−1670.
(7) Oostenbrink, C.; Villa, A.; Mark, A. E.; Van Gunsteren, W. F. *J. Comput. Chem.* **2004**, *25*, 1656−1676.
(8) Jorgensen, W. L.; Tirado-Rives, J. *Proc. Natl. Acad. Sci . U. S. A.* **2005**, *102*, 6665−6670.
(9) Mobley, D. L.; Liu, S.; Cerutti, D. S.; Swope, W. C.; Rice, J. E. *J. Comput.-Aided. Mol. Des.* **2011**, *26*, 551−562.
(10) Nicholls, A.; Mobley, D. L.; Guthrie, J. P.; Chodera, J. D.; Bayly, C. I.; Cooper, M. D.; Pande, V. S. *J. Med. Chem.* **2008**, *51*, 769−779.
(11) Guthrie, J. P.; Povar, I. *Can. J. Chem.* **2009**, *87*, 1154−1162.
(12) Moult, J. *Curr. Opin. Struct. Biol.* **2005**, *15*, 285−289.
(13) Mobley, D. L.; Dumont, E.; Chodera, J. D.; Dill, K. A. *J. Phys. Chem. B* **2007**, *111*, 2242−2254.
(14) Paluch, A. S.; Mobley, D. L.; Maginn, E. J. *J. Chem. Theory Comput.* **2011**, *7*, 2910−2918.
(15) Schmid, N.; Eichenberger, A. P.; Choutko, A.; Riniker, S.; Winger, M.; Mark, A. E.; Van Gunsteren, W. F. *Eur. Biophys. J.* **2011**, *40*, 843−856.
(16) Mobley, D. L.; Dumont, E.; Chodera, J. D.; Dill, K. A. *J. Phys. Chem. B* **2007**, *111*, 2242−2254.
(17) Vanommeslaeghe, K.; Hatcher, E.; Acharya, C.; Kundu, S.; Zhong, S.; Shim, J.; Darian, E.; Guvench, O.; Lopes, P.; Vorobyov, I.; MacKerell, A. D., Jr. *J. Comput. Chem.* **2010**, *31*, 671−690.
(18) Price, M. L. P.; Ostrovsky, D.; Jorgensen, W. L. *J. Comput. Chem.* **2001**, *22*, 1340−1352.
(19) Klauda, J. B.; Brooks, B. R. *J. Chem. Theory Comput.* **2008**, *4*, 107−115.
(20) Wang, J.; Wolf, R. M.; Caldwell, J. W.; Kollman, P. A.; Case, D. A. *J. Comput. Chem.* **2004**, *25*, 1157−1174.
(21) Martin, M. G.; Siepmann, J. I. *J. Phys. Chem. B* **1998**, *102*, 2569−2577.
(22) Wick, C. D.; Martin, M. G.; Siepmann, J. I. *J. Phys. Chem. B* **2000**, *104*, 8008−8016.
(23) Rai, N.; Bhatt, D.; Siepmann, J. I.; Fried, L. E. *J. Chem. Phys.* **2008**, *129*, 194510.
(24) Wick, C. D.; Stubbs, J. M.; Rai, N.; Siepmann, J. I. *J. Phys. Chem. B* **2005**, *109*, 18974−18982.
(25) Martin, M. G.; Siepmann, J. I. *J. Phys. Chem. B* **1999**, *103*, 4508−4517.
(26) Shivakumar, D.; Williams, J.; Wu, Y.; Damm, W.; Shelley, J.; Sherman, W. *J. Chem. Theory Comput.* **2010**, *6*, 1509−1519.
(27) Morgantinit, P.-Y.; Kollman, P. A. *J. Am. Chem. Soc.* **1995**, *117*, 6057−6063.
(28) Mobley, D. L.; Bayly, C. I.; Cooper, M. D.; Shirts, M. R.; Dill, K. A. *J. Chem. Theory Comput.* **2009**, *5*, 350−358.
(29) Price, D. J.; Brooks, C. L. *J. Comput. Chem.* **2005**, *26*, 1529−1541.
(30) Rizzo, R. C.; Aynechi, T.; Case, D. A.; Kuntz, I. D. *J. Chem. Theory Comput.* **2006**, *2*, 128−139.
(31) Ghosh, A.; Rapp, C. S.; Friesner, R. A. *J. Phys. Chem. B* **1998**, *102*, 10983−10990.
(32) Gallicchio, E.; Zhang, L. Y.; Levy, R. M. *J. Comput. Chem.* **2002**, *23*, 517−529.
(33) Caleman, C.; van Maaren, P. J.; Hong, M.; Hub, J. S.; Costa, L. T.; Van der Spoel, D. *J. Chem. Theory Comput.* **2012**, *8*, 61−74.
(34) Jakalian, A.; Jack, D. B.; Bayly, C. I. *J. Comput. Chem.* **2002**, *23*, 1623−1641.
(35) Jämbeck, J. P. M.; Mocci, F.; Lyubartsev, A. P.; Laaksonen, A. *J. Comput. Chem.* **2013**, *34*, 187−97.
(36) Klimovich, P. V; Mobley, D. L. *J. Comput.-Aided. Mol. Des.* **2010**, *24*, 307−316.
(37) Lyubartsev, A. P.; Martsinovski, A. A.; Shevkunov, S. V.; Vorontsov-Velyaminov, P. N. *J. Chem. Phys.* **1992**, *96*, 1776−1783.
(38) Aberg, K. M.; Lyubartsev, A. P.; Jacobsson, S. P.; Laaksonen, A. *J. Chem. Phys.* **2004**, *120*, 3770−3776.
(39) Lyubartsev, A. P.; Laaksonen, A.; Vorontsov-Velyaminov, P. N. *Mol. Phys.* **1994**, *82*, 455−471.
(40) Lyubartsev, A. P.; Førrisdahl, O. K.; Laaksonen, A. In *Proceedings of the 2nd International Conference on Natural Gas Hydrates*; Toulouse, France, June 2−6, 1996; pp 311−318.
(41) Lyubartsev, A. P.; Jacobsson, S. P.; Sundholm, G.; Laaksonen, A. *J. Chem. Phys. B* **2001**, *105*, 7775−7782.
(42) Lyubartsev, A. P.; Laaksonen, A. *Comput. Phys. Commun.* **2000**, *128*, 565−589.
(43) Ahmed, A.; Sandler, S. I. *J. Chem. Phys.* **2012**, *136*, 154505.
(44) Lyubartsev, A.; Laaksonen, A. *MDynaMix Package Version 5.2.4 User Manual*; Stockholm University: Stockholm, Sweden, 2011.
(45) Rai, N.; Siepmann, J. I. *J. Phys. Chem. B* **2007**, *111*, 10790−10799.
(46) ParamChem. https://www.paramchem.org/AtomTyping/ (accessed May 05, 2012).

(47) Vanommeslaeghe, K.; Raman, E. P.; MacKerell, A. D., Jr. *J. Chem. Inf. Model.* **2012**, *52*, 3155−3168.
(48) Vanommeslaeghe, K.; MacKerell, A. D., Jr. *J. Chem. Inf. Model.* **2012**, *52*, 3144−3154.
(49) Breneman, C. M.; Wiberg, K. B. *J. Comput. Chem.* **1990**, *11*, 361−373.
(50) Vanquelef, E.; Simon, S.; Marquant, G.; Garcia, E.; Klimerak, G.; Delepine, J. C.; Cieplak, P.; Dupradeau, F.-Y. *Nucleic Acids Res.* **2011**, *39*, W511−W517.
(51) Dupradeau, F.-Y.; Pigache, A.; Zaffran, T.; Savineau, C.; Lelong, R.; Grivel, N.; Lelong, D.; Rosanski, W.; Cieplak, P. *Phys. Chem. Chem. Phys.* **2010**, *12*, 7821−7839.
(52) Thompson, J. D.; Kelly, C. P.; Lynch, B. J.; Xidos, J. D.; Li, J.; Hawkins, G. D.; Zhu, T.; Volobuev, Y.; Dupuis, M.; Rinaldi, D.; Liotard, D. A.; Cramer, C. J.; Truhlar, D. G. *SMxGauss version 3.3*; University of Minnesota: Minneapolis, MN, 2007.
(53) Abraham, M. H.; Whiting, G. S.; Fuchs, R.; Chambers, E. J. *J. Chem. Soc., Perkin Trans. 2* **1990**, 291−300.
(54) Adamo, C.; Barone, V. *J. Chem. Phys.* **1998**, *108*, 664−675.
(55) Frisch, M. J.; Trucks, G. W.; Schlegel, H. B.; Scuseria, G. E.; Robb, M. A.; Cheeseman, J. R.; Scalmani, G.; Barone, V.; Mennucci, B.; Petersson, G. A.; Nakatsuji, H.; Caricato, M.; Li, X.; Hratchian, H. P.; Izmaylov, A. F.; Bloino, J.; Zheng, G.; Sonnenberg, J. L.; Hada, M.; Ehara, M.; Toyota, K.; Fukuda, R.; Hasegawa, J.; Ishida, M.; Nakajima, T.; Honda, Y.; Kitao, O.; Nakai, H.; Vreven, T.; Montgomery, J. A., Jr.; Peralta, J. E.; Ogliaro, F.; Bearpark, M.; Heyd, J. J.; Brothers, E.; Kudin, K. N.; Staroverov, V. N.; Kobayashi, R.; Normand, J.; Raghavachari, K.; Rendell, A.; Burant, J. C.; Iyengar, S. S.; Tomasi, J.; Cossi, M.; Rega, N.; Millam, J. M.; Klene, M.; Knox, J. E.; Cross, J. B.; Bakken, V.; Adamo, C.; Jaramillo, J.; Gomperts, R.; Stratmann, R. E.; Yazyev, O.; Austin, A. J.; Cammi, R.; Pomelli, C.; Ochterski, J. W.; Martin, R. L.; Morokuma, K.; Zakrzewski, V. G.; Voth, G. A.; Salvador, P.; Dannenberg, J. J.; Dapprich, S.; Daniels, A. D.; Farkas, O.; Foresman, J. B.; Ortiz, J. V; Cioslowski, J.; Fox, D. J. *Gaussian 09 User's Reference*; Gaussian Inc.: Wallingford CT, 2010.
(56) Dunning, T. H., Jr. *J. Chem. Phys.* **1971**, *55*, 716−723.
(57) Jakalian, A.; Bush, B. L.; Jack, D. B.; Bayly, C. I. *J. Comput. Chem.* **2000**, *21*, 132−146.
(58) Case, D. A.; Darden, T. A.; Cheatham, T. E.; Simmerling, C. L.; Wang, J.; Duke, R. E.; Luo, R.; Walker, R. C.; Zhang, W.; Merz, K. M.; Roberts, B.; Hayik, S.; Roitberg, A.; Seabra, G.; Swails, J.; Goetz, A. W.; Kolossváry, I.; Wong, K. F.; Paesani, F.; Vanicek, J.; Wolf, R. M.; Liu, J.; Wu, X.; Brozell, S. R.; Steinbrecher, T.; Gohlke, H.; Cai, Q.; Ye, X.; Hsieh, M.-J.; Cui, G.; Roe, D. R.; Mathews, D. H.; Seetin, M. G.; Salomon-Ferrer, R.; Sagui, C.; Babin, V.; Luchko, T.; Gusarov, S.; Kovalenko, A.; Kollman, P. A. *AmberTools 1.5*; University of California: San Francisco, CA, 2010.
(59) Jorgensen, W. L.; Chandrasekhar, J.; Madura, J. D.; Impey, R. W.; Klein, M. L. *J. Chem. Phys.* **1983**, *79*, 926−935.
(60) Wu, Y.; Tepper, H. L.; Voth, G. A. *J. Chem. Phys.* **2006**, *124*, 024503.
(61) Hoover, W. G. *Phys. Rev. A* **1985**, *31*, 1695−1697.
(62) Nosé, S. *J. Chem. Phys.* **1984**, *81*, 511−519.
(63) Ewald, P. P. *Ann. Phys.* **1921**, *369*, 253−287.
(64) Allen, M. P.; Tildesley, D. J. *Computer Simulation of Liquids*; Oxford University Press: New York, 1989.
(65) Jämbeck, J. P. M.; Mocci, F.; Lyubartsev, A. P.; Laaksonen, A. *J. Comput. Chem.* **2012**, 1−11.
(66) Yang, L.; Ahmed, A.; Sandler, S. I. *J. Comput. Chem.* **2012**, *34*, 284.
(67) Abraham, M. H.; Ibrahim, A.; Zissimos, A. M. *J. Chromatogr., A* **2004**, *1037*, 29−47.
(68) Marenich, A. V; Kelly, C. P.; Thompson, J. D.; Hawkins, G. D.; Chambers, C. C.; Giesen, D. J.; Winget, P.; Cramer, C. J.; Truhlar, D. G. *Minnesota Solvation Database*, version 2007; University of Minnesota: Minneapolis, MN, 2009.
(69) Kelly, C. P.; Cramer, C. J.; Truhlar, D. G. *J. Chem. Theory Comput.* **2005**, *1*, 1133−1152.
(70) Koch, W.; Holthausen, M. C. *A Chemist's Guide to Density Functional Theory*; Wiley-VCH: Weinheim, Germany, 2000; p 294.
(71) Ben-Naim, A.; Marcus, Y. *J. Chem. Phys.* **1984**, *81*, 2016−2027.
(72) Ashcraft, R. W.; Raman, S.; Green, W. H. *J. Phys. Chem. B* **2007**, *111*, 11968−11983.
(73) Katritzky, A. R.; Oliferenko, A. A.; Oliferenko, P. V.; Petrukhin, R.; Tatham, D. B. *J. Chem. Inf. Comput. Sci.* **2003**, *43*, 1794−1805.
(74) Abraham, M. H. *Chem. Soc. Rev.* **1992**, *096*, 73−83.
(75) Katritzky, A. R.; Oliferenko, A. A.; Oliferenko, P. V.; Petrukhin, R.; Tatham, D. B. *J. Chem. Inf. Comput. Sci.* **2003**, *43*, 1806−1814.
(76) Bordner, A. J.; Cavasotto, C. N.; Abagyan, R. A. *J. Phys. Chem. B* **2002**, *106*, 11009−11015.
(77) Lewin, J.; Rai, N.; Maerzke, K.; Bhatt, D.; Siepmann, J.; Maiti, A.; Fried, L. In *Energetic Materials*; CRC Press: Boca Raton, FL, 2010; pp 63−76.
(78) Kelly, C. P.; Cramer, C. J.; Truhlar, D. G. *Theor. Chem. Acc.* **2005**, *113*, 133−151.
(79) Walsh, M. E.; Jenkins, T. F.; Thorne, P. G. *J. Energ. Mater.* **1995**, *13*, 357−383.
(80) Shirts, M. R.; Pande, V. S. *J. Chem. Phys.* **2005**, *122*, 134508.
(81) Fennell, C. J.; Dill, K. A. *J. Stat. Phys.* **2011**, *145*, 209−226.
(82) Shivakumar, D.; Deng, Y.; Roux, B. *J. Chem. Theory Comput.* **2009**, *5*, 919−930.
(83) MacCallum, J. L.; Tieleman, D. P. *J. Comput. Chem.* **2003**, *24*, 1930−1935.
(84) Boyer, R. D.; Bryan, R. L. *J. Phys. Chem. B* **2012**, *116*, 3772−3779.